Laser cooling and trapping
of neutral atoms

Y. Castin, J. Dalibard and C. Cohen-Tannoudji

Laboratoire de Spectroscopie Hertzienne de l'E.N.S.*

et Collège de France

24, rue Lhomond, F-75231 Paris Cedex 5, France

The aim of this lecture is to present a simple review of the basic physical processes allowing one to control, with laser beams, the velocity and the position of neutral atoms. The control of the velocity corresponds to a cooling of atoms, i.e. to a reduction of the atomic velocity spread around a given value. The control of the position means a trapping of atoms in real space. The best present performances will be given, in terms of the lowest temperatures and the highest densities. The corresponding highest quantum degeneracy will also be estimated. It is imposed by fundamental limits, which will be briefly described.

This lecture will also give the general trends of the field, the new directions which look like promising for observing quantum statistical effects in laser cooled atomic samples, but which are for the moment restricted by unsolved problems.

1   Introducing the simple schemes

The radiative forces acting on atoms in a light field can be split into two parts, a reactive one and a dissipative one. The dissipative force (radiation pressure), which involves basically scattering processes, is velocity dependent. We will see that this dependence leads to the Doppler cooling scheme and to the concept of optical molasses, and we will give the corresponding minimal achievable temperature. The dissipative force can be made position dependent, through a gradient of magnetic field, so that the atoms are also trapped, in the so-called magneto-optical trap.

---

*Unité de recherche de l'Ecole Normale Supérieure et de l'Université Paris 6, associée au CNRS

1.1 Effect of light on the atomic internal state

Since the atoms in laser cooling are illuminated by quasi-resonant light, they can be considered as two-level atoms, with a metastable state g, called "ground state" in what follows, and an excited state e. The transition between g and e has a resonant frequency ω_A and an electric dipole d. The excited state can decay by spontaneous emission with a rate Γ. In this section, we consider the simple case of atoms with no sublevels in the ground state g. The influence of the presence of Zeeman sublevels in g on laser cooling is the subject of §2.

The laser electric field is a superposition of travelling waves of frequency ω_L close to ω_A and of complex amplitude $\mathcal{E}_0$. An important parameter is $\delta = \omega_L - \omega_A$, detuning of the laser frequency ω_L from the atomic frequency ω_A. The dipolar coupling between atom and light leads to a time dependent amplitude of transition from g to e, noted $(\Omega/2)e^{-i\omega_L t}$, and from e to g, $(\Omega^*/2)\,e^{i\omega_L t}$. The parameter $\Omega = -d\mathcal{E}_0/\hbar$ is called the Rabi frequency. The amplitude of transition can be made time independent by the following time dependent unitary transformation $S(t)$ changing the excited state:

$$S(t) = e^{i\omega_L t|e\rangle\langle e|} \tag{1}$$

which gives to the $|g\rangle \longrightarrow |e\rangle$ transition the effective Bohr frequency $\omega_A - \omega_L = -\delta$ instead of ω_A. This leads to the time independent effective hamiltonian H_{eff} for the evolution of the internal atomic state:

$$H_{\text{eff}} = \hbar \begin{pmatrix} -\delta - i\Gamma/2 & \Omega/2 \\ \Omega^*/2 & 0 \end{pmatrix} \tag{2}$$

This matrix is given in the $\{|e\rangle, |g\rangle\}$ basis and the $-i\Gamma/2$ term accounts for the instability of the excited state.

The effect of the coupling will be considered in the perturbative regime:

$$s = \frac{|\Omega|^2/2}{\delta^2 + \Gamma^2/4} \ll 1 \tag{3}$$

The dimensionless quantity s is called the saturation parameter and gives the relative amount of time spent by the atoms in the excited state. In this regime, one of the eigenvectors of H_{eff} remains close to g, with the eigenvalue $\hbar(\delta - i\Gamma/2)s/2$. The corresponding real part $\hbar\delta' = \hbar\delta s/2$ is the signature of a reactive effect: it describes the shift of the energy of the ground state by the incoming light (light shift). The imaginary part is the signature of a dissipative effect: the ground state g becomes unstable by contamination by the excited state through the Rabi coupling; the corresponding rate $\Gamma' = \Gamma s/2$ is the excitation rate of the ground state by the laser light. Note that the following discussion can be generalised to arbitrary laser intensities (see e.g. the so-called "dressed atom" picture in [1]).

1.2   Effect of light on the atomic external state

In contrast to the internal atomic variables, which correspond to the electronic motion relative to the nucleus, the external variables are related to the motion of the atomic center of mass; the important ones for laser cooling are the position $\vec{r}$ and the momentum $\vec{p}$ of the atom. These external variables are also changed by the interaction with the laser light. For example, the momentum $\vec{p}$ shifts to $\vec{p} \pm \hbar\vec{k}$ after the absorption or the emission of one photon of momentum $\hbar\vec{k}$. The corresponding atomic recoil velocity $\hbar k/M$, where M is the mass of the atom, is an important parameter in laser cooling, as we shall see; it is on the order of 3 mm/s for cesium. The effect of light on atomic motion can be described in terms of radiative forces. These forces can be dissipative or reactive, depending on the contribution or the non contribution of the momentum of spontaneously emitted photons.

For the simple case of an atom in a plane running wave, the dissipative force corresponds to the usual radiation pressure; it is due to the absorption of one laser photon of momentum $\hbar\vec{k}_L$ and the spontaneous emission of one fluorescence photon of momentum $\hbar\vec{k}_S$. The corresponding average change in atomic momentum is $\langle \delta\vec{p} \rangle = \langle \hbar\vec{k}_L - \hbar\vec{k}_S \rangle = \hbar\vec{k}_L$; the mean contribution of $\hbar\vec{k}_S$ is zero because spontaneous emission occurs with the same probability in two opposite directions. The mean radiative force is then simply $\hbar\vec{k}_L$ times the rate of absorption-spontaneous emission cycles. This rate, on the order of $\Gamma s/2$ at low saturation, cannot exceed $\Gamma/2$ at high saturation. The dissipative force thus saturates at high laser intensity to $\hbar k_L \Gamma/2$, a limit almost 10^4 higher than the gravitational force Mg for cesium.

The reactive forces derive from an effective potential, which is the position dependent light shift of the atomic level g; it is due to successive absorption-stimulated emission cycles. Consider for example the light shift U of the atomic ground state in the vicinity of a gaussian laser beam. When the laser light is detuned to the red ($\delta < 0$), $U(\vec{r})$ is negative and maximal in absolute value in the laser beam, and close to 0 out of the laser beam. The effect of $U(\vec{r})$ is thus a trapping of the atoms around the maxima of intensity of the laser light. This has been used to make a trap, at a detuning large enough for the dissipative effects (heating due to spontaneous emission) to be negligible [2]. An improved version of the optical trap, using stabilisation by radiative pressure forces, is presented in [3].

1.3   Doppler cooling and the Doppler limit

The Doppler cooling scheme has been proposed independently by Hänsch and Schawlow, Wineland and Dehmelt in 1975 [4, 5]. It strongly relies on
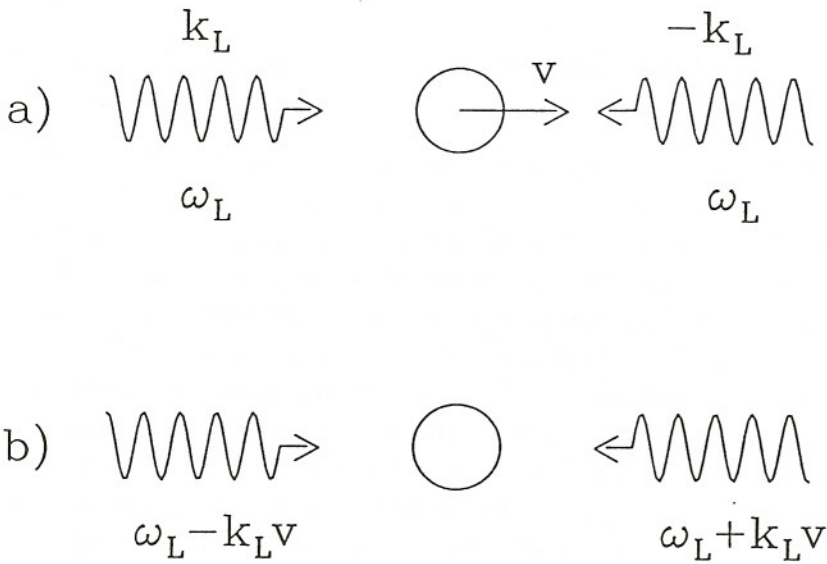
Figure 1: *The laser waves of the Doppler cooling configuration, in the lab (a) and in the atomic rest frame (b).*

the atomic velocity dependence of the radiation pressure due to the Doppler effect. In this scheme, the cooling of the atomic velocity along a given direction z is obtained by the superposition of two counterpropagating running waves along z. The two waves have the same weak amplitude $\mathcal{E}_0$ and the same frequency ω_L, detuned to the red $(\delta = \omega_L - \omega_A < 0)$. Consider an atom of velocity $\vec{v}$, and call $\vec{k}$ the wave vector of the laser wave copropagating with the atom $(\vec{k} \cdot \vec{v} > 0)$. In the atomic rest frame, this wave has an apparent frequency $\omega_L - \vec{k} \cdot \vec{v} < \omega_L < \omega_A$, so it is moved farther from resonance by the Doppler effect $-\vec{k} \cdot \vec{v}$. The counterpropagating wave, with wave vector $-\vec{k}$, is on the contrary put closer to resonance by the Doppler effect $(\vec{k} \cdot \vec{v} > 0)$. (see Figure 1). The atom will then absorb photons preferentially in the counterpropagating wave, so that it feels a mean radiative force opposed to its velocity along z. This force vanishes for an atom at rest, and can be shown to behave as a linear friction force:

$$F_z = -\alpha v_z \tag{4}$$

where α is a friction coefficient, for slow enough atoms. Cooling is provided along the other directions x and y by use of two additional standing waves. The corresponding light field acts as a viscous medium on atomic motion, the so-called "optical molasses"[6].

Spontaneous emission plays an essential role in the cooling mechanism: it allows the dissipation of energy by emission of fluorescence photons with a frequency $\omega_S > \omega_L$. However, the random momentum recoil of the atoms after spontaneous emission is responsible for a heating, i.e. an increase of the mean atomic kinetic energy, which can be described, as in standard brownian

4

motion theory, by a momentum diffusion coefficient D:

$$\frac{d}{dt}\langle p_i^2\rangle\Big|_{\text{heating}} = 2D \qquad i = x, y, z \tag{5}$$

This heating can counterbalance the effect of the damping force:

$$\frac{d}{dt}\langle p_i^2\rangle\Big|_{\text{cooling}} = -\frac{2\alpha}{M}\langle p_i^2\rangle \qquad i = x, y, z \tag{6}$$

so that an equilibrium is reached. The corresponding stationary velocity distribution is gaussian, with an effective temperature T given by Eintein's law:

$$k_B T = \frac{D}{\alpha} \tag{7}$$

where k_B is the Boltzmann constant. After an explicit derivation of α and D from the two-level atom model, one finds that the minimal temperature T_D, called the Doppler limit, is obtained for a detuning $\delta = -\Gamma/2$ and is given by [7, 8]:

$$k_B T_D = \frac{\hbar\Gamma}{2} \tag{8}$$

It corresponds to $T_D = 120\ \mu\text{K}$ for cesium atoms.

1.4   The magneto-optical trap (MOT)

The effect of Doppler cooling is a compression in momentum space, but it has no confining effect in real space, the atoms performing simply a spatial diffusive random walk in the optical molasses. In order to trap the atoms in real space, the radiation pressure is made also position dependent via a gradient of magnetic field.

The principle of the MOT can be explained with the following model (see Figure 2). Consider an atomic transition occurring between a ground state of angular momentum $j_g = 0$ and an excited state of angular momentum $j_e = 1$. Atoms are excited by two counterpropagating laser waves which are respectively σ_+ and σ_- polarized along z. The fact that the excited state has several Zeeman sublevels $|e, m = -1\rangle_z$, $|e, m = 0\rangle_z$ and $|e, m = 1\rangle_z$, of angular momentum $m\hbar$ along z, is essential. First, these sublevels undergo different Zeeman shifts due to the external magnetic field, say $-\mu B, 0$ and μB respectively for a magnetic field B along the quantization axis z, $\mu > 0$ being proportional to the magnetic dipole moment in the excited state. Second, the ground state is coupled to $|e, 1\rangle$ only by absorption of photons in the σ_+ laser wave, and to $|e, -1\rangle$ only by absorption of photons in the σ_- laser wave. Suppose now that B varies linearly along z and vanishes in $z = 0$. An atom at rest in $z = 0$ sees no mean radiative force, the two laser beams being

exactly equally detuned far from resonance. In $z > 0$ however, because of the Zeeman shifts, the resonance frequency for the $|g,0\rangle \longleftrightarrow |e,1\rangle$ transition is larger than ω_A, and is smaller than ω_A for the $|g,0\rangle \longleftrightarrow |e,-1\rangle$ transition. The σ_- laser wave is then closer to resonance than the σ_+ laser wave, and the atom at rest feels a net radiative force pushing it towards $z = 0$. The conclusion is reversed for negative values of z. In this configuration, there is thus, in addition to the damping force, a trapping force, linear with z around $z = 0$, so that the net mean radiative force along z reads:

$$F_z = -\alpha v_z - \kappa z \qquad (9)$$

The atomic motion is damped in an effective external harmonic potential, and the atomic cloud gets a finite spatial extension given in steady state by:

$$\kappa \langle z^2 \rangle = k_B T = \frac{D}{\alpha} \qquad (10)$$

The first experimental demonstration of the MOT has been reported in [9].
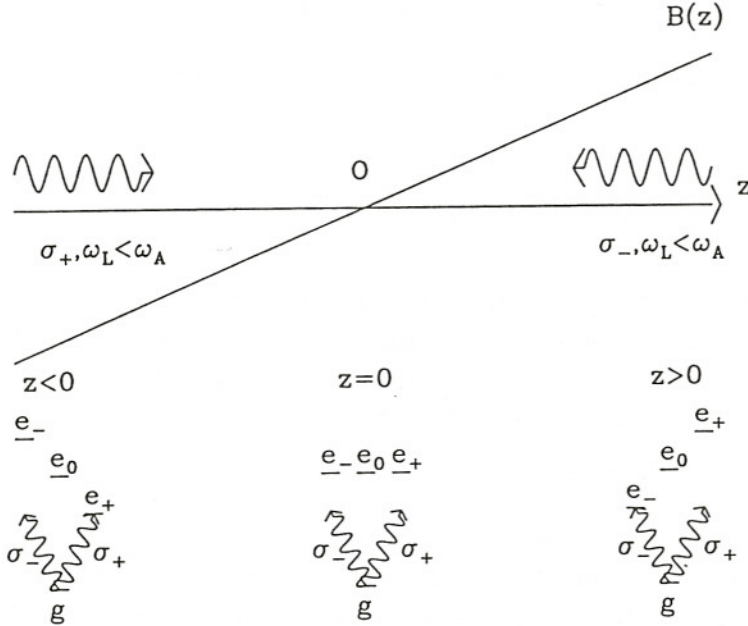
Figure 2: *The principle of the magneto-optical trap on a $j_g = 0 \rightarrow j_e = 1$ transition.*

2   Beating the Doppler limit

Since 1988, precise experimental measurements of the temperatures of optical molasses have been performed [10, 11, 12, 13, 14, 15, 16]. The lowest temperatures are found to be well below the Doppler limit (8). On a heavy

atom like cesium, the lowest measured temperatures are on the order of 3 μK, a factor 40 smaller than the Doppler limit, and are observed at large atom-laser detuning: $|\delta| \gg \Gamma$, instead of $\delta = -\Gamma/2$ as expected from the Doppler cooling theory. All these results are experimental evidence of very efficient new cooling mechanisms.

These mechanisms have been identified theoretically on simple 1D models [17, 18]. They strongly rely on the existence of several degenerate sublevels in the atomic state g, a feature left out in the two-level atom model used for Doppler cooling but present in experimental optical molasses, because of the hyperfine and Zeeman structures of the atomic ground state. A second important feature is the spatial variation of the laser field polarization at the optical wavelength scale, a condition which is automatically fulfilled in 3D laser configurations, and which is obtained in the simple 1D models by giving different polarizations to the two counterpropagating waves.

In this section, we will analyse in some details only one of the presently known polarization gradient cooling mechanisms, relying on the so-called "Sisyphus effect"[17]. The corresponding minimal kinetic energies no longer scale as $\hbar\Gamma$, as for Doppler cooling, but as the recoil energy $E_R = \hbar^2 k^2/2M$, i.e. the mean increase of the atomic kinetic energy after the spontaneous emission of a single photon. Note that E_R is well below the Doppler limit $\hbar\Gamma/2$ for the typical atomic transitions used in optical molasses. In the case of cesium atoms, for example, $\hbar\Gamma/2$ is one thousand times larger than the recoil energy. In this very cold regime, it has been predicted theoretically and checked experimentally that quantization of atomic motion plays an important role in Sisyphus cooling. This has led to a new picture for the laser cooled atomic samples, the so-called "optical lattices".

2.1   Optical pumping and light shifts

As seen in §1.1 for the two-level atom case in the low saturation regime, the effect of light on the internal atomic state is to shift the energy levels (reactive effect) and to give a finite lifetime to the ground state (dissipative effect). When the atom has several Zeeman sublevels in the ground state, the reactive effect can lead to different light shifts of the sublevels, and the dissipation effect can lead to real transitions between the various sublevels, through optical pumping cycles [19].

The last two features play an important role in laser cooling. They are present in the simple 1D scheme depicted in Figure 3. The light field is obtained by superposition of two coherent counterpropagating running waves along z, with the same amplitude $\mathcal{E}_0$ and frequency ω_L, but with orthogonal

linear polarizations. For an appropriate phase choice, the total electric field is given by:

$$\vec{\mathcal{E}}(z,t) = \vec{\mathcal{E}}^+(z)e^{-i\omega_L t} + \text{c.c} \qquad (11)$$

$$\vec{\mathcal{E}}^+(z) = \mathcal{E}_0 \left[\vec{e}_x e^{ikz} - i\vec{e}_y e^{-ikz} \right] \qquad (12)$$

where $\vec{e}_x$, $\vec{e}_y$ are unit vectors along x and y. One can check that the polarization of $\vec{\mathcal{E}}(z,t)$ depends on z, with a periodicity $\lambda_{\text{opt}}/2$, where $\lambda_{\text{opt}} = 2\pi/k$ is the optical wavelength. For example, in $z = 0$, $\lambda_{\text{opt}}/2$, ..., $\vec{\mathcal{E}}(z,t)$ is σ_- circularly polarized along z; it is σ_+ polarized in $z = \lambda_{\text{opt}}/4$, $3\lambda_{\text{opt}}/4$, ...; it is linearly polarized along $(\vec{e}_x - \vec{e}_y)/\sqrt{2}$ in $z = \lambda_{\text{opt}}/8$, $5\lambda_{\text{opt}}/8$, ... and along $(\vec{e}_x + \vec{e}_y)/\sqrt{2}$ in $z = 3\lambda_{\text{opt}}/8$, $7\lambda_{\text{opt}}/8$.

Consider an atom with an angular momentum $j_g = 1/2$ in the ground state and an angular momentum $j_e = 3/2$ in the excited state. This atom is illuminated by the previous field configuration, with a laser frequency ω_L below the resonance frequency ω_A:

$$\delta = \omega_L - \omega_A < 0 \qquad (13)$$

The transition amplitudes between the atomic energy levels of given angular momentum along z, $\{|g,m\rangle, m = \pm 1/2\}$ and $\{|e,m'\rangle, m' = \pm 3/2, \pm 1/2\}$, by absorption or stimulated emission of laser photons are now weighted by the appropriate Clebsch-Gordan coefficients (see Figure 4a) and thus depend on the polarization of the electric field.
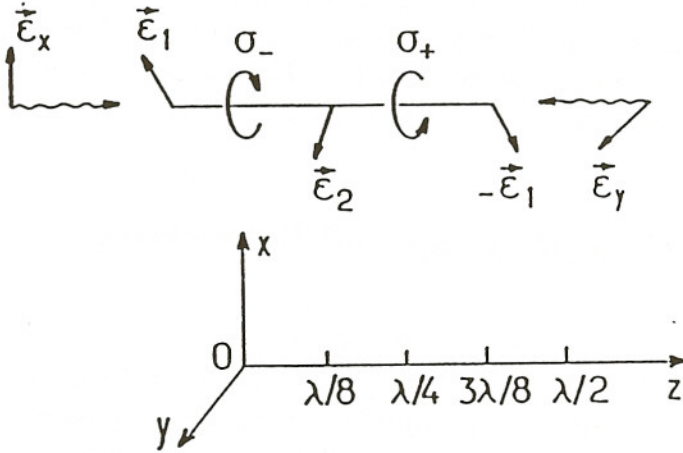
Figure 3: *Resulting electric field in the $x - y$ laser configuration.*

In a place where the light is purely σ_- polarized, the $|g,-1/2\rangle$ sublevel is coupled to the electric field with an amplitude $\sqrt{3}$ larger than the $|g,+1/2\rangle$ sublevel. It therefore experiences a light shift 3 times larger, $\hbar\delta s$ instead of $\hbar\delta s/3$ for $|g,+1/2\rangle$), with a saturation parameter s given by (3) [1]. In the

---

[1] At first sight, there seems to be a discrepancy of a factor 2 between the light shift (and also the excitation rate) derived here and the one given in §1.1. In fact, in $z = 0$, the electric field amplitude is $\sqrt{2}\mathcal{E}_0$, instead of $\mathcal{E}_0$ in §1.1.

presence of pure σ_- light, the sublevel $|g, -1/2\rangle$ has not only a well defined light shift, but is also a trap for the internal atomic state. It is coupled by laser light only to the $|e, -3/2\rangle$ excited state sublevel, which by spontaneous emission can only decay to $|g, -1/2\rangle$. If the atom is initially in the $|e, +3/2\rangle$ excited sublevel, it is eventually put in the $|g, +1/2\rangle$ ground sublevel by spontaneous emission. If the atom is initially in the $\{|g, +1/2\rangle, |e, -1/2\rangle\}$ manifold, it is put back in $|g, +1/2\rangle$ after a spontaneous emission with a probability $1/3$ (σ_- emission) and it is trapped into $|g, -1/2\rangle$ with a probability $2/3$ (linearly polarized emission along z). The population in $|g, +1/2\rangle$ therefore tends exponentially to zero for an increasing number of fluorescence cycles. The corresponding transition rate from $|g, +1/2\rangle$ to $|g, -1/2\rangle$ by the optical pumping mechanism is found to be $\Gamma s \cdot 1/3 \cdot 2/3 = 2\Gamma s/9$.

In a place when the light is purely σ_+ polarized, the situation is reversed between the sublevels. The atoms are now put by optical pumping in the $|g, +1/2\rangle$ sublevel, which undergoes the largest light shift. The present configuration exhibits therefore a strong correlation between the spatial modulation of light shifts and the spatial modulation of optical pumping rates. For a negative atom-laser detuning δ, the optical pumping rates are everywhere the largest from the highest energy ground state sublevel to the lowest one.

2.2   Sisyphus cooling mechanism

We now explain how cooling occurs in the previously described atom-laser configuration. The key point is that the position dependent light shifts of the sublevels $|g, \pm 1/2\rangle$ appear as effective potentials $U_\pm(z)$ for a moving atom. It will be thus convenient to introduce the mechanical energies $E_\pm = Mv^2/2 + U_\pm(z)$, where v is the atomic velocity along z.

A typical trajectory in $(z, E_\pm)$ space is shown in Figure 4b. It starts in the sublevel $|g, -1/2\rangle$, in a minimum of $U_-(z)$, with a kinetic energy larger than the modulation depth:

$$U_0 = -\frac{2}{3}\hbar\delta s \tag{14}$$

of the potential. If the optical pumping time τ_p from $|g, -1/2\rangle$ to $|g, +1/2\rangle$ is long enough, the atom can climb the potential hill and reach the top of $U_-(z)$ before changing its internal state. During this part of the motion, the mechanical energy E_- remains constant and there is a conversion of kinetic energy into potential energy. In the vicinity of the maxima of $U_-(z)$, the laser light is σ_+ polarized and the atom has there the maximal probability to be optically pumped into the $|g, +1/2\rangle$ sublevel, by absorption of a laser photon followed by a spontaneous emission. If such a process takes place, the atom

9

is put back into a valley, but for the $U_+(z)$ potential this time. The resulting decrease of potential energy leads to a corresponding excess of energy for the spontaneously emitted photon with respect to $\hbar\omega_L$. Dissipation of energy thus originates in this cooling scheme from the spontaneous emission of anti-Stokes Raman photons.
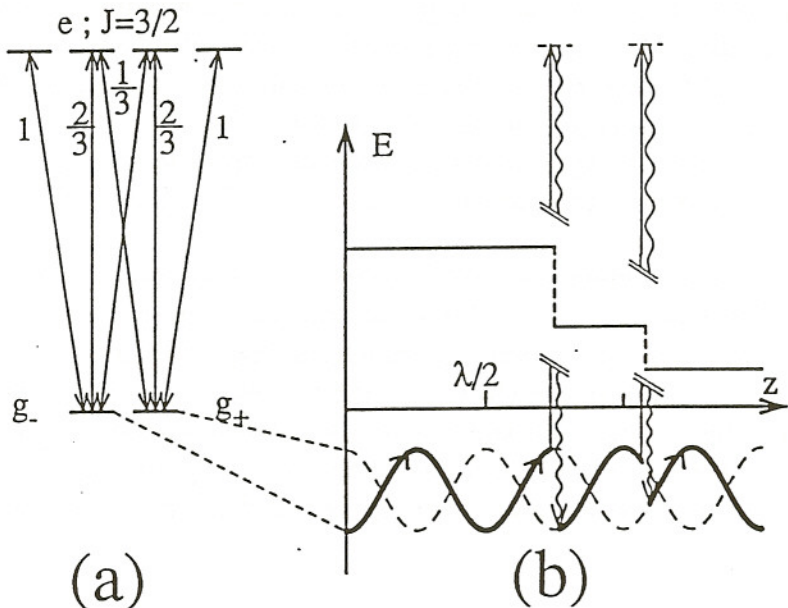
Figure 4: *a) Atomic-level scheme and intensity factors (square of the Clebsch-Gordan coefficients) for a $j_g = 1/2 \rightarrow j_e = 3/2$ atomic transition. b) In the Sisyphus cooling configuration, the position dependent light shifts of the ground state sublevels and a typical atomic trajectory in the position-energy space.*

The atoms therefore do not stop climbing potential hills, as Sisyphus did in the greek mythology, until their kinetic energy becomes on the order of the modulation depth U_0. This intuitive reasoning is confirmed by a theoretical analysis, close to the one used already for Doppler cooling, which introduces a friction coefficient α and a momentum diffusion coefficient D, as in brownian motion theory. The derivation of the coefficient D and α leads to the equilibrium temperature given in [17]:

$$k_B T = \frac{\langle p^2 \rangle}{M} \propto U_0 \sim -\hbar \delta s \qquad (15)$$

2.3 Limit of Sisyphus cooling

The equilibrium temperature given in the previous section is proportional to the laser intensity, and scales as $1/|\delta|$, for large detunings ($|\delta| \gg \Gamma$). This

10

has been confirmed experimentally in 3D on a wide range of detunings and laser intensities, and for several atomic species [15, 16]. The precise value of the slope for the 3D experiments cannot of course be deduced from the simple 1D model that we described. Actually, such a scaling law for Sisyphus cooling cannot be realistic for any values of the parameters. For example, it leads to a vanishing equilibrium temperature in the limit of vanishing laser intensity. In this regime of very small light shifts, the experimental results are indeed deviating from (15).

In order to have a more complete understanding of Sisyphus cooling, one has to take into account carefully the heating of the atoms due to random recoil after spontaneous emission. The Sisyphus effect, corresponding to a decrease of the potential energy on the order of U_0 after an optical pumping cycle, is then counterbalanced by an increase of the kinetic energy on the order of the recoil energy $E_R = \hbar^2 k^2 / 2M$. Cooling works only when U_0 is above a threshold of a few E_R, and the minimal achievable temperature is expected from (15) to scale as the recoil energy E_R.

The precise value of the Sisyphus cooling limit has been derived from a quantum treatment of both the internal atomic state and the atomic motion in laser light, for the presented simple 1D model [20]. For a given atom-laser detuning δ/Γ, the dependence of the steady state kinetic energy on the modulation depth U_0 of the potential is shown in Figure 5. The scaling law $k_B T \sim U_0$ is recovered in the limit of large U_0/E_R. The existence of a threshold on U_0 corresponds to a rapid increase of the average kinetic energy, when U_0/E_R becomes too small. The smallest possible value of the root mean square atomic momentum is on the order of 5.5 $\hbar k$, reached for $U_0 \sim 100 E_R$ in the limit of large detunings $|\delta| \gg \Gamma$.

2.4 Quantization of atomic motion in the optical potential wells

It has been found fruitful to try to get more insight into the coldest regime of Sisyphus cooling. One can check that in this regime, the following inequality holds:

$$\Omega_{\text{osc}} \tau_p \gg 1 \qquad (16)$$

where $\Omega_{\text{osc}} \sim k\sqrt{U_0/M}$ is the oscillation frequency of the atoms in the bottom of the potential wells, and $\tau_p \sim 1/\Gamma s$ is the optical pumping time. This leads to a level spacing $\sim \hbar\Omega_{\text{osc}}$ for the quantized atomic motion in $U_\pm(z)$ much larger than the radiative width $\hbar/\tau_p$ of these levels due to optical pumping.

Therefore a good basis for the analysis of the cooling is provided by the
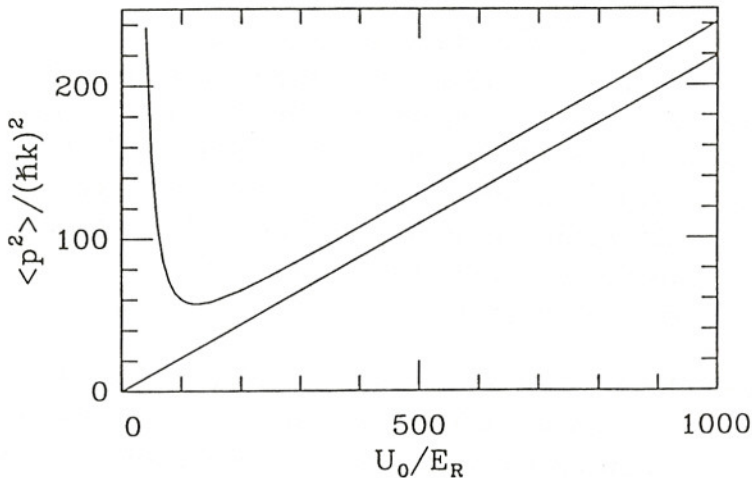
Figure 5: *In a full quantum treatment of Sisyphus cooling, mean kinetic energy $\langle p^2 \rangle / 2M$ in units of recoil energy $E_R = \hbar^2 k^2 / 2M$ as a function of the modulation depth U_0 of the optical potential wells in units of E_R. The atom-laser detuning is $\delta = -5\Gamma$.*

stationary solutions of the Schrödinger equation for the atomic motion in $U_\pm(z)$ [21]. Since the potentials $U_\pm(z)$ are periodic, of period $\lambda_{\mathrm{opt}}/2$, the corresponding energy spectrum has a band structure. The lowest energy bands, corresponding to quasi-harmonic motion in the bottom of the potential wells (see Figure 6 taken from [22]), have a negligible tunnel width. On the contrary, the energy gaps become very small for the quasi-free motion well above the potential hills. The effect of optical pumping in this basis can be described simply by transition rates between the various energy levels, when inequality (16) holds. The corresponding rate equations allow one to calculate the steady state populations of the energy bands. The maximal population in the most populated band $v = 0$ is found to be 0.34 in [21], for $U_0 \simeq 60 E_R$.

The existence of well resolved external quantum levels in 1D Sisyphus cooling has been demonstrated experimentally. A probe laser beam, with a very small intensity, is sent through the optical molasses along the direction of the laser cooling beams. Two side-bands are clearly observed on the probe absorption spectrum, for a probe frequency $\omega_p = \omega_L \pm \Omega_{\mathrm{osc}}$. They correspond to stimulated Raman transitions between two successive vibrational levels in the potential wells. Since the lowest level is the most populated one, Raman cycles starting with atoms in $v = 0$ are expected to be dominant. When ω_p is below ω_L ($\omega_p \simeq \omega_L - \Omega_{\mathrm{osc}}$), the dominant process is therefore the absorption of one photon in the cooling beams followed by a stimulated emission of one photon in the probe beam, and the probe beam is amplified. When ω_p is above ω_L ($\omega_p \simeq \omega_L + \Omega_{\mathrm{osc}}$), the Raman processes are mainly the absorption of one photon in the probe beam followed by the stimulated emission of one photon in the cooling beams, and the probe beam is absorbed
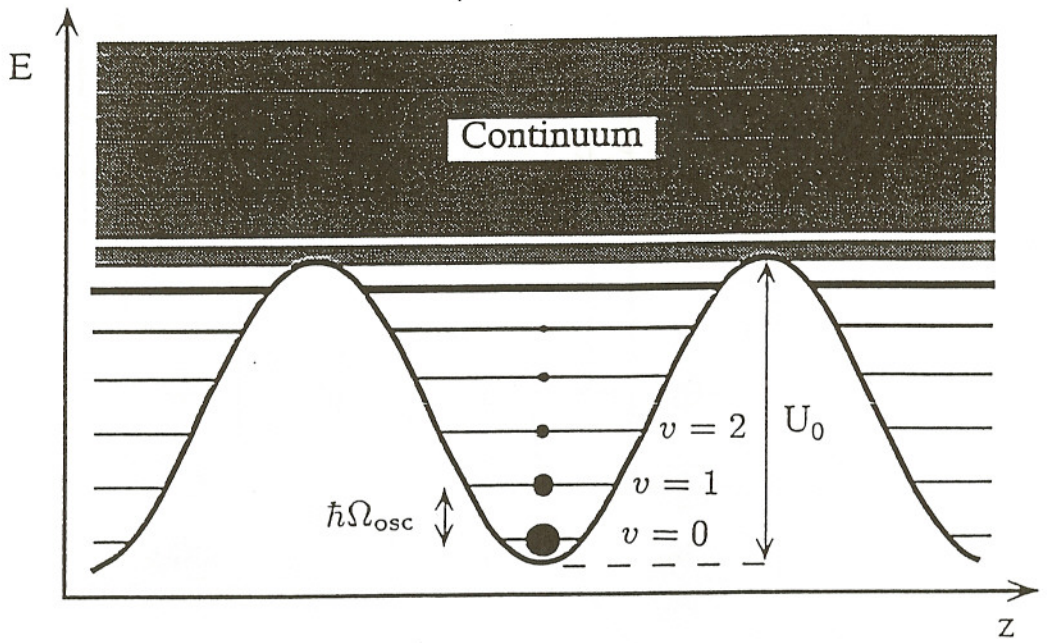
Figure 6: *Band structure of the energy spectrum for the quantum motion in $U_+(z)$ optical potential wells. The vibrational levels are labelled $v = 0, 1, ...$ The dark circular areas are proportional to the steady state populations of the vibrational levels.*

(see Figure 7 taken from [22]). The so-called "overtones" (Raman transitions with $\delta v = 2$, $\delta v = 3, ...$) can also be identified. A stimulated Rayleigh line is also observed at $\omega_p = \omega_L$; it can be shown to give evidence for a spatial antiferromagnetic order of the atoms [23, 24]. These experiments are the first observations of quantized external levels of a neutral atom in an optical field. An important point is that about half of the atoms are expected to be in minimum uncertainty states [22]. These observations have been confirmed by studies of the fluorescence spectra of 1D optical molasses [25].

2.5 Optical lattices in 2D and 3D

In the preceeding sections, we have seen that 1D Sisyphus cooling in a laser field can lead to a strong accumulation of the atoms around the points where the field is circularly polarized. Such a property can be generalized to 2D and 3D.

Theoretical results are available in 2D [26, 27]. The quantum approach is similar to the one used in 1D. In the frame of this lecture, the main results concern the population of the energy levels in steady state. They are found to be strongly reduced: the maximum population of the deepest band shifts from 0.34 in 1D to 0.09 in 2D. This does not mean that cooling is less efficient in 2D, but it is simply a signature of degeneracy effects among the vibrational
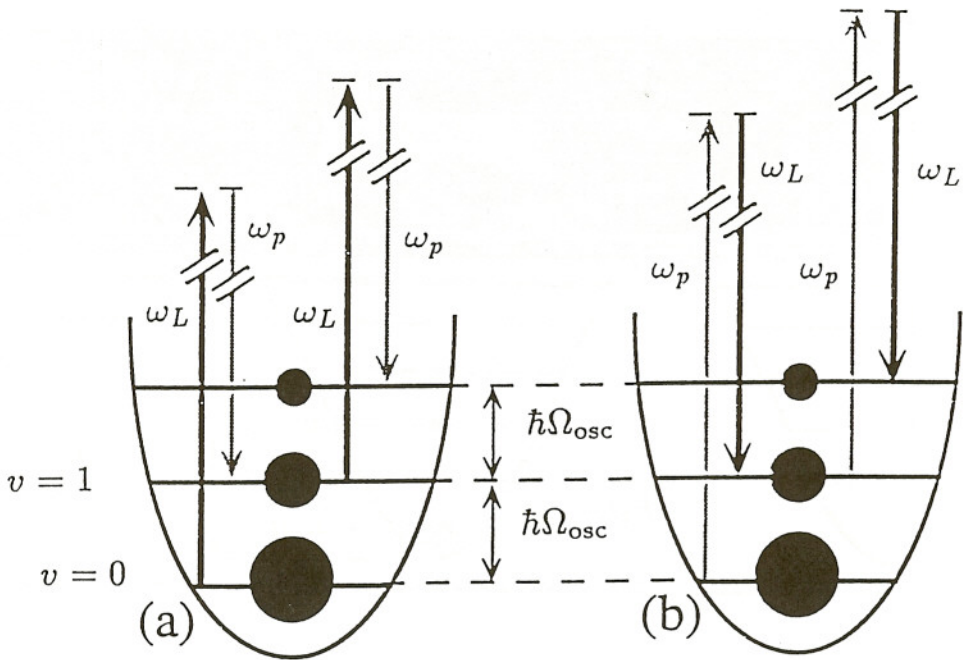
Figure 7: *Examples of Raman processes induced between the atomic vibrational levels by a weak probe beam of frequency ω_p sent through the 1D optical molasses. The populations of the energy levels are represented by dark areas. On fig.a, the Raman processes lead to an amplification of the probe beam ($\omega_p \simeq \omega_L - \Omega_{osc}$). On fig.b, the Raman processes lead to an absorption of the probe beam ($\omega_p \simeq \omega_L + \Omega_{osc}$).*

levels. Let us indeed consider the atomic motion in the bottom of the 2D potential wells. It is found to be almost harmonic, and the energy bands are labelled by the two quantum numbers n_x and n_y of the corresponding 2D isotropic harmonic oscillator. If the motions along x and y are considered as decoupled, the probability of finding the atoms in the ground state $|n_x = 0, n_y = 0\rangle$ of their motion is the product of the probabilities of finding them in the ground states $|n_x = 0\rangle$ and $|n_y = 0\rangle$ of their motion along x and y respectively. This simple reasoning leads to the estimate:

$$\Pi^{2D}_{n_x=n_y=0} \simeq \left(\Pi^{1D}_{n=0}\right)^2 \tag{17}$$

not far from the exact results.

To get experimental evidence for vibrational levels in $\sigma_\pm$ optical potential wells, one has to get rid of phase fluctuations between the orthogonal running waves, in order to avoid distorsion of the electric field polarization away from $\sigma_\pm$ in the minima of the wells. This has been realized in München, with 2 and 3 orthogonal standing waves with well controlled phases [28, 29]. In Paris, an alternative to this approach has been developped. The idea is to use in nD the minimal number of running waves leading to cooling, which is $n + 1$. In this case, as it is evident for the particular case $n = 1$, the periodic pattern

of potential wells is only shifted by phase fluctuations. A hexagonal lattice in 2D, and a cubic body centered lattice in 3D have been obtained, and have been analysed by a probe beam [30].

All these results lead to a completely different physical picture of the laser cooled atomic samples. The concept of optical molasses is replaced by the one of optical lattices, which consist of periodic arrays of microtraps, with vibrational levels for the atomic motion. This description is well suited to the discussion of statistical effects, the quantum degeneracy (i.e. the population of the most populated state of the one-atom density matrix) being derived simply from the population of the lowest energy band. However, these optical lattices are for the moment quite lacunar, only a few percent of the sites being occupied. In order to increase the quantum degeneracy, one has to increase the atomic density, thanks to an extra trapping mechanism.

2.6   Experimental results on the magneto-optical trap

The geometry of the magneto-optical trap has been described on a simple 1D model in §1.4. It can be extended to a 3D configuration in the following way. The magnetic field gradient is provided by two coaxial coils travelled by opposite electric currents. Close to $\vec{r} = \vec{0}$, where the resulting magnetic field is vanishing, one has the approximate spatial dependence for $\vec{B}$:

$$\vec{B}(\vec{r}) \simeq \frac{b_0}{a}(-x/2, -y/2, z) \tag{18}$$

Three pairs of counterpropagating σ_+ and σ_- circularly polarized laser waves, along x, y and z, provide 3D trapping and cooling in the presence of the magnetic gradient. Note that the laser beams propagating along z and perpendicularly to z have opposite helicities, because magnetic field gradients are of opposite signs along z and x, y.

Experimental studies of the magneto-optical trap for atoms in a cell have given evidence for two different regimes (see for example [31] for cesium atoms).

First, a low density regime, with a density n less than 10^{10} atoms/cm^3, is obtained when a small number N of atoms (up to 10^6) are present in the trap. The important point is then that the temperatures in the trap are the same (down to 3 μK) than the ones measured in the $\sigma_+ - \sigma_-$ optical molasses in the absence of magnetic field. The sub-Doppler cooling mechanisms, which strongly rely on the light shifts of the various Zeeman ground sublevels, are thus not destroyed by the magnetic field in the trap [32, 33, 31, 34]. This is due to the fact that the trapping mechanism accumulates the atoms in a

small region around $\vec{B} = \vec{0}$. The corresponding minimal radii of the atomic cloud in the trap are found experimentally to be on the order of 40 μm, for a magnetic field gradient of 10 gauss/cm.

When a large number N of atoms are present in the trap (up to $3 \cdot 10^8$), a high density regime is observed, with maximal densities n around $3 \cdot 10^{12}$ atoms/cm^3. However, the temperatures in the trap are found then to be higher than the ones in the $\sigma_+ - \sigma_-$ optical molasses, the corresponding excess of temperature ΔT scaling simply as $N^{1/3}$ for a given laser detuning and intensity. The highest quantum degeneracies in the trap are actually not obtained at the highest densities.

In order to estimate this quantum degeneracy, we suppose that the mean number of atoms in the most populated quantum levels inside the trap is given by:

$$\Pi_{\mathrm{max}} = n \Lambda_{\mathrm{DB}}^3 \quad \text{with} \quad \Lambda_{\mathrm{DB}} = \frac{h}{\sqrt{2\pi M k_{\mathrm{B}} T}} \tag{19}$$

This formula, valid only for a gas of non interacting particles in thermal equilibrium in the low degeneracy regime, is found to be in reasonably good agreement, when transposed to the 2D case, with the theoretical results mentioned in §2.5. At the moderate density $n = 8 \cdot 10^{11}$ atoms/cm^3 and quite low temperature $T = 10\mu$K, a situation which is a compromise between the search for low temperatures and high densities in the trap, equation (19) leads to a degeneracy Π_{max} on the order of 10^{-4}.

We now give a qualitative account of the collective effects responsible for the limits on the maximal densities n and the corresponding temperatures T achievable in the magneto-optical trap.

At long range, the exchange of fluorescence photons between atoms leads to a repulsive force, proportional to the flux of photons emitted from one of the atoms through a fictitious surface located around the other atom and of area σ_A, the resonant absorption cross section. It thus scales as $1/r_{12}^2$, where r_{12} is the distance between the two atoms. This force has a mean antitrapping effect, which limits the compression in real space of the atomic cloud by the trap. It also fluctuates, which introduces extra heating and increases the temperature [35, 36]. Fortunately, the effect of this long range interaction should be reduced at high laser detuning.

At short range (i.e. for r_{12} smaller than the optical wavelength λ_{opt}), the dipolar interaction between an atom in excited state and an atom in ground state has non negligible effects. It shifts the energy levels by an amount on the order of the natural width $\hbar\Gamma$ of the excited state, for $r_{12} \sim \lambda_{\mathrm{opt}}/2\pi$. Such a shift is larger than the light shifts leading to the low laser intensity Sisyphus effect and can destroy the cooling mechanism. At high atomic densities, it

can lead to the formation of molecules, with a loss term of atoms from the trap scaling as n^2 [37, 38].

The existence of such strong atomic interactions in the presence of laser light thus leads to the following intuitive conclusion, that the density in the magneto-optical trap cannot exceed a value such that the mean distance between atoms becomes smaller than λ_{opt}, which leads to a maximal density n given by

$$n\lambda_{\text{opt}}^3 \sim 1 \qquad (20)$$

This corresponds to $n \sim 2 \cdot 10^{12}$ atoms/cm^3 on cesium, on the order of the experimental results.

3 Beating the recoil limit

One of the conclusions of the previous section was that it seemed difficult, in the presence of quasi-resonant laser light of wavelength λ_{opt}, to achieve so high atomic densities n that $n\lambda_{\text{opt}}^3 \gg 1$, while keeping the very low temperatures realized at low densities. In the search for quantum degeneracy, the regime where the atomic de Broglie wavelength λ_{DB} is much larger than the optical wavelength λ_{opt} is thus particularly interesting. In this case, the parameter $n\lambda_{\text{DB}}^3$ can be on the order of unity, with still $n\lambda_{\text{opt}}^3$ being very small, so that collisional effects between atoms should remain small.

This interesting regime is called "subrecoil", because the condition $\lambda_{\text{DB}} = h/\Delta p \gg \lambda_{\text{opt}}$ implies an equilibrium temperature $T = \Delta p^2/Mk_{\text{B}}$ much smaller than the so-called recoil temperature $T_{\text{R}} = \hbar^2 k^2/Mk_{\text{B}}$, where $k = 2\pi/\lambda_{\text{opt}}$. The problem is that subrecoil temperatures cannot be reached by the "usual" cooling scheme described in the previous sections. In these schemes, indeed, spontaneous emission of fluorescence photons, which is essential for carrying away the atomic mechanical energy, never stops. The atoms thus continuously experience random recoils of size $\hbar k$ in momentum space, so that the equilibrium temperature cannot be much smaller than the recoil temperature.

In section §3.1, we present a 1D subrecoil cooling scheme called "velocity selective coherent population trapping" [39, 40]. It is not the only one in the laser cooling field. Another scheme has been shown experimentally to beat the recoil limit [41], and there are also several theoretical proposals [42, 43]. The general idea of all these schemes is however the same: it consists of accumulating the atoms into states very weakly coupled to laser light and with a very narrow width in momentum space. The fundamental limits of subrecoil cooling adressed in §3.2 can thus be considered as being quite

general.

3.1 1D velocity selective coherent population trapping

Consider the so-called "Λ type" atomic system illuminated by two mutually coherent laser waves, of opposite wave vectors $k\vec{e_z}$ and $-k\vec{e_z}$ along z and of same frequency ω_L, but with orthogonal circular polarizations, respectively σ_+ and σ_- (see Figure 8). We describe in a quantum manner the atomic motion along z by introducing the external states $|p\rangle$ corresponding to the plane waves of momentum $p\vec{e_z}$. The atomic dynamics can then be analysed as follows [40].
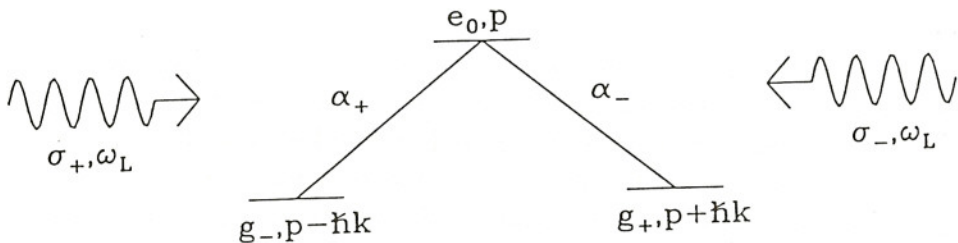
Figure 8: *The Λ atomic system in the $\sigma_+ - \sigma_-$ laser configuration. In the absence of spontaneous emission, note the existence of closed families of atomic states labelled by p, atomic momentum along z in the excited state.*

In the absence of spontaneous emission, an atom initially in the state $|e_0, p\rangle$, i.e. in the internal (electronic) state $|e_0\rangle$ and with a center of mass motion of momentum p along z, is coupled only to $|g_-, p-\hbar k\rangle$ (by stimulated emission of a photon in the σ_+ wave), with an amplitude α_+, and to $|g_+, p+\hbar k\rangle$ (by stimulated emission of a photon in the σ_- wave), with an amplitude α_-. The space of atomic states can then be split into a direct sum of an infinite number of closed families $\mathcal{F}(p) = \{|e_0, p\rangle, |g_-, p - \hbar k\rangle, |g_+, p + \hbar k\rangle\}$ labelled by p. Since there is only one internal excited state $|e_0\rangle$ for two ground levels $|g_\pm\rangle$, we can form, inside each family $\mathcal{F}(p)$, a particular linear combination $|\psi_{NC}(p)\rangle$ non coupled to the laser:

$$|\psi_{NC}(p)\rangle = \frac{1}{\sqrt{|\alpha_+|^2 + |\alpha_-|^2}}[\alpha_-|g_-, p - \hbar k\rangle - \alpha_+|g_+, p + \hbar k\rangle] \qquad (21)$$

Note that this combination is not a stationary state, because it has no well defined kinetic energy:

$$(p - \hbar k)^2 \neq (p + \hbar k)^2 \qquad (22)$$

except for the particular case $p = 0$, for which $|\psi_{NC}\rangle$ is a perfectly trapping state, called "dark state".

Let us now take into account spontaneous emission. Starting from $|e_0, p\rangle$, the atom now eventually decays into $|g_\pm, p - p_z^S\rangle$, where p_z^S is the momentum of the fluorescence photon along z and is randomly distributed between $-\hbar k$ and $+\hbar k$. Spontaneous emission thus couples family $\mathcal{F}(p)$ to the "neighbouring" families $\mathcal{F}(p')$, with $p' = p \pm \hbar k - p_z^S$ in the range $[p - 2\hbar k, p + 2\hbar k]$. This random change of p after a fluorescence cycle may transfer the atoms into the dark state $|\psi_{NC}(0)\rangle$ or into a quasi dark state for p very close to 0, where they remain trapped and where they pile up. The corresponding effect on the atomic momentum distribution is to produce two peaks at $p = \pm\hbar k$, because $|\psi_{NC}(0)\rangle$ is a superposition of states of momenta $+\hbar k$ and $-\hbar k$. The width of these peaks is not limited by the recoil momentum $\hbar k$, but scales as $1/\sqrt{t}$, where t is the atom-laser interaction time, at it has been checked numerically in [40]. For an idea of the proof and an analysis of the height of the peaks as function of time, we refer to [44].

3.2 Experimental results below the recoil limit

The 1D cooling scheme introduced in §3.1 has been demonstrated experimentally on metastable helium [39], on a transition between a ground state of angular momentum $j_g = 1$ and an excited state of angular momentum $j_e = 1$. To see why the Λ structure of §3.1 is an acceptable model in this geometry, let us introduce the internal atomic states of angular momentum $m\hbar$ around z, $\{|g, m\rangle_z, |e, m\rangle_z, m = 0, \pm 1\}$. Since the laser electric field has no component along z, the V system, formed by $\{|e, -1\rangle_z, |g, 0\rangle_z, |e, 1\rangle_z\}$, and the Λ system $\{|g, -1\rangle_z, |e, 0\rangle_z, |g, 1\rangle_z\}$ are not coherently coupled. The key point is then that the excited sublevel of the Λ system $|e, 0\rangle_z$ cannot decay by spontaneous emission into $|g, 0\rangle_z$, because the corresponding $\Delta m = 0$ Clebsch-Gordan coefficient is vanishing. Therefore, after a few spontaneous emissions from the excited sublevels of the V system, $|e, \pm 1\rangle_z$, the atoms are pumped into the Λ system, from which they cannot escape.

Experimental results on the atomic momentum distribution after an interaction time $t = 350\Gamma^{-1}$, where $\hbar\Gamma$ is the natural width of the excited state, are sketched on Figure 9. The two peaks in $\pm\hbar k$ are visible, above the initial momentum distribution. Their half width at half maximum δp allows one to define an effective temperature [2] T_{eff} on the order of 0.5 recoil temperature T_R. Note that the velocity selective coherent population trapping can

---

[2]More precisely, δp is defined as the half width of the peaks at the relative height $e^{-1/2}$, so that the equation $T_{\text{eff}} = \delta p^2/M$ defining T_{eff} as a function of δp is exact for a Maxwell-Boltzmann distribution.

be generalized on a $j_g = 1 \rightarrow j_e = 1$ transition to multidimensional cooling [40, 45, 46]. A 2D experiment is in progress on helium in Paris.
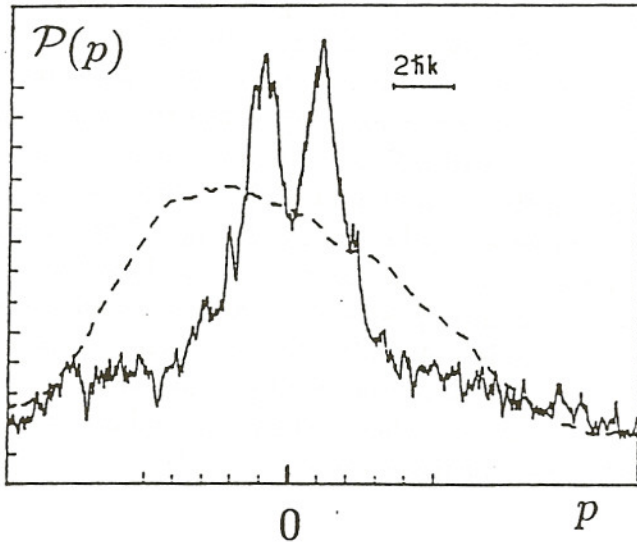
Figure 9: *Experimental results on the momentum distribution for 1D subrecoil cooling. The two peaks of the final distribution in $\pm \hbar k$ (solid line) are above the initial distribution (dashed line).*

As mentioned in the introductory remarks of this section, another subrecoil cooling scheme has been demonstrated experimentally [41]. Stimulated Raman transitions, between two hyperfine ground states $|1\rangle$ and $|2\rangle$, are produced by two counterpropagating synchronized laser pulses and provide a high selectivity in atomic velocity. The atoms whose velocity v meets the Raman resonance condition $v = v_0$ are transferred into $|2\rangle$ by the pulses and are then "pushed" towards zero velocity back into $|1\rangle$ through a pumping resonant travelling wave. Successive cooling cycles of this type are then performed, with a scanning of v_0 from high velocities towards low velocities, in order to collect most of the atoms. Since v_0 is always different from 0, there is a small region around $v = 0$ where the atoms never meet the Raman resonance condition, and where they pile up. Very sharp momentum distributions around $p = 0$ have thus been obtained and observed in 1D, with effective temperatures down to $T_R/10$.

3.3 The limits of subrecoil cooling

In order to get observable effects depending on the quantum statistics of the atoms, it is necessary to provide three dimensional cooling. For the moment, there is no experimental evidence of an efficient velocity selective coherent

population trapping in 3D or even in 2D. In the low density regime, new theoretical methods have been developped to try to predict the evolution of the effective temperature as a function of the interaction time [44]. They rely on Monte-Carlo wave function simulations, describing quantum mechanically both the internal and external atomic state. This procedure has first the advantage to use much smaller objects than the full atomic density matrix ρ in 2D or 3D (a discretized wave function has $\mathcal{N}$ components, whereas ρ has $\mathcal{N}^2$ components). Since it deals with stochastic objects, it has also allowed a connection with efficient tools of statistical physics, the so-called Lévy flights [47]. The maximal atomic density one can achieve without destroying the darkness of the trapping state by multiple photon scattering between atoms is still an open question.

The subrecoil cooling schemes have also to face the severe problem of gravity. Indeed, the atoms in the trapping state feel no radiative force, so that the gravitational force can put them out of the dark state and make them fall down! A first possible solution to this problem is to try to counterbalance gravity by a non dissipative force, by using for example the very non resonant dipolar trap mentioned in §1.2. One can also perform cooling in a free falling frame. This has been done already, for ordinary optical molasses, in an airplane in parabolic flight [48].

A different and promising type of solution is adressed in the next section. The idea is to use gravity as an ally, for making a trap, instead of trying to get rid of it.

4   What next ?

As explained in §3, the presently known subrecoil cooling schemes cannot be efficiently applied in 3D because of gravity. In this section, we explain how to get an atomic cavity by using gravity and a parabolic atomic mirror (§4.1). A quantum picture for the atomic motion inside this cavity is briefly given in §4.2: as light waves do in usual laser cavities, matter waves have well defined modes in the gravitational cavity, and one may hope to get quantum statistical effects if several atoms occupy the same quantum modes.

4.1   A gravitational atomic cavity

The realization of an atomic cavity requires a non dissipative bounding of the atomic motion in all directions.

Bounding of vertical motion can be obtained through a horizontal plane atomic mirror. The principle of such a device has been given in [49]. By total internal reflection of a travelling laser wave inside a piece of glass, an evanescent wave is produced in the vacuum above the glass, with an intensity $I(z)$ exponentially decreasing with increasing z. When the laser frequency ω_L is larger than the atomic resonance frequency ω_A, the atomic ground state experiences in vacuum a positive light shift, which is a decreasing function of z and thus gives rise to a repulsive potential for the atoms. The laser is detuned far from resonance so that dissipative effects during reflection are small: fluorescence cycles indeed have a rate scaling as $I/(\omega_L - \omega_A)^2$. However, ω_L has to be not too far from resonance, so that the laser has a high enough intensity to provide reactive effects (i.e. light shifts, proportional to $I/(\omega_L - \omega_A)$) able to reflect the atoms. This last condition is very restrictive for thermal atomic velocities, and in this case only reflection for grazing atomic incidence is observed [50]. On the contrary, it is easily fulfilled after use of the laser cooling techniques, and reflection under normal atomic incidence can then be obtained [51].

In order to bound also the transverse atomic motion, the plane mirror of the previous scheme is replaced by a parabolic mirror, with an evanescent wave still present at its surface. The atoms are released with negligible initial velocities from a switched-off magneto-optical trap and bounce off the evanescent wave (see Figure 10). The corresponding classical orbits are paraxial and are shown to be stable [52]. Experimental realizations are in progress in Paris (at the ENS) and in Gaithersburg (at NIST). Recent observation of about ten bounces has been reported in Paris, for cesium atoms, with the following experimental evidence. At a time t after the drop of the atoms, a probe beam is sent through a small volume δV around the initial position of the atomic cloud, and the fluorescence light is collected. This procedure gives a signal proportional to the number $N(t)$ of atoms in the volume δV. Such a measurement is destructive, because atoms are pushed away and heated by the probe beam, so that the whole process has to be restarted from the beginning, if one wants to get $N(t')$ at a different time t'. The result of numerous such cycles is shown in Figure 11 (see [53]; less recent results, with only four bounces, are given in [54]).

4.2   Towards degeneracy effects in the cavity

When the atomic motion is treated quantum mechanically, the dynamics in the cavity is analogous to the one of light in an optical cavity. The corresponding quantum modes for the matter waves have been investigated theoretically [52]. They correspond mathematically to the stationary solutions
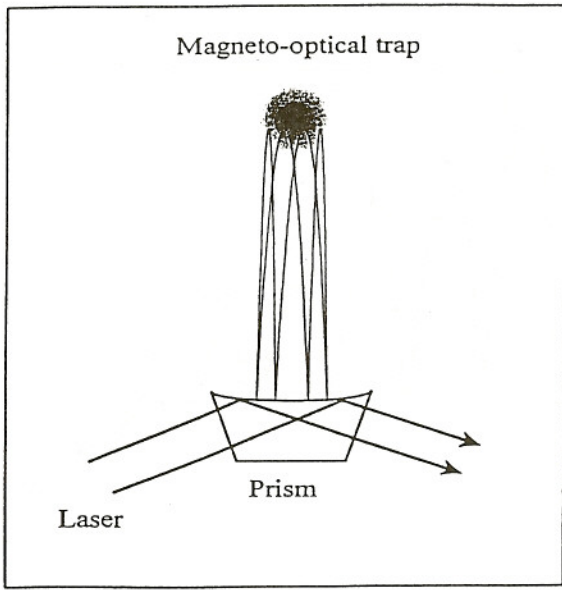
Figure 10: *Principle and loading of the atomic gravitational cavity.*

of the Schrödinger equation for the atomic wave function $\psi(\vec{r}, t)$:

$$i\hbar\partial_t\psi = -\frac{\hbar^2}{2M}\Delta\psi + Mgz\psi \tag{23}$$

$$\psi(\vec{r}, t) = \phi(\vec{r})e^{-iEt/\hbar} \tag{24}$$

with appropriate boundary conditions, responsible for the discrete nature of the allowed energies E. In an idealized model, the atomic mirror is considered as a perfect one, and ψ is required to vanish on the surface of the mirror. The problem is then readily separated in parabolic coordinates, so that one can solve separately for "transverse" and "vertical" motions. As an illustrative example, a vertical cut of the probability distribution in real space $|\phi(\vec{r})|^2$ is given in Figure 12. The numerous horizontal node lines indicate a highly excited vertical motion. On the contrary, the transverse motion is in the ground state. Estimates of the density of modes in the cavity for realistic experimental conditions are discussed in [52].

The basic idea to get statistical effects in the gravitational cavity is simply the hope to put several (bosonic!) atoms in the same quantum mode. It appears to be more promising to try to populate a highly excited mode rather than the ground ones. Such a mode has indeed a much larger spatial volume, so that the atomic density in real space is lower and collisional effects are reduced, for a given quantum degeneracy. The way of filling one particular mode of the cavity is still a difficult open question. One has to find efficient selective processes, and the subsequent atomic dynamics, far from thermal equilibrium, should be close to the one of photons in a laser cavity, rather than to the one of the Bose-Einstein condensation.
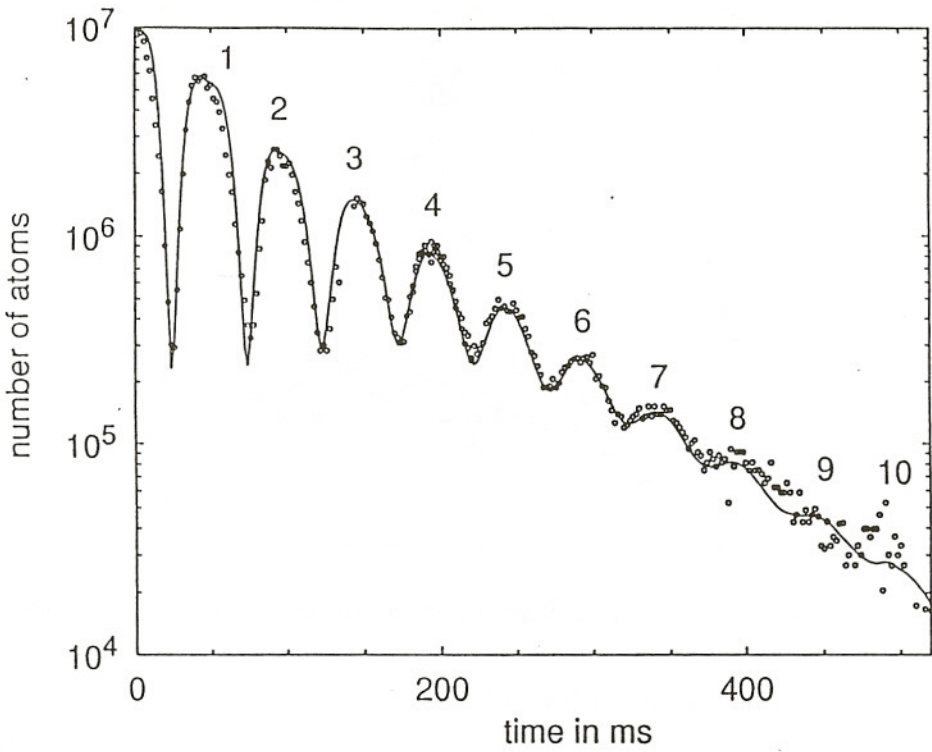
Figure 11: *The number of atoms in the gravitational cavity in Paris is measured as a function of time using the fluorescence induced by a probe beam (cf. text). The points on the figure give the number of atoms in the probe beam for different times after their release. The curve is a fit calculated by a Monte-Carlo simulation. The successive bounces are labelled 1,2...*
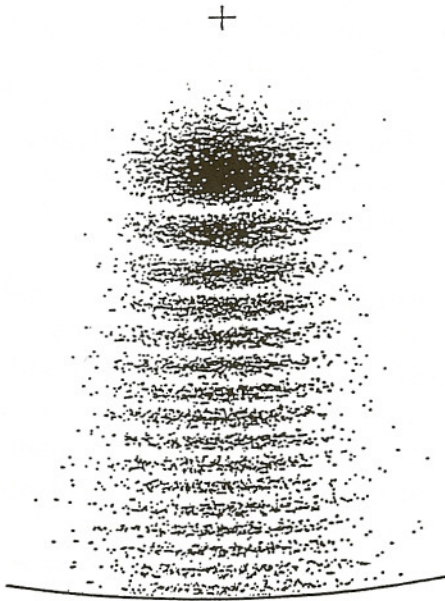
Figure 12: *The calculated probability distribution in real space of a mode in the gravitational atomic cavity. The cross corresponds to the focus of the parabolic surface of the mirror.*

5 Conclusion

In this lecture, we have given first a brief survey of nowadays quite standard techniques in the laser cooling field. Ultracold atomic samples are obtained in optical molasses, optical lattices and in the magneto-optical traps, but quantum degeneracy remains small, for the following fundamental reasons. Collective effects, such as the dipolar interaction between atoms in ground and excited states, prevent from reaching densities n much larger than $1/\lambda_{\mathrm{opt}}^3$, where λ_{opt} is the optical wavelength. On the other hand, the spontaneously emitted photons limit the maximal atomic de Broglie wavelength λ_{DB} to a few $\lambda_{\mathrm{opt}}/10$, so that $n\lambda_{\mathrm{DB}}^3$ should not be much larger than 10^{-3}.

We have also described some of the new potentialities offered by laser manipulation of atoms in the search for quantum degeneracies.

First, subrecoil cooling could beat the previous simple reasoning. It leads to de Broglie wavelengths larger than the optical wavelength, so that condition $n\lambda_{\mathrm{DB}}^3 \sim 1$ could be satisfied with still $n\lambda_{\mathrm{opt}}^3 \ll 1$. However, one has to find a way to counterbalance gravity, and more detailed investigations of the effect of multidimensionality are required.

Second, the search for degeneracy effects among the highly excited states of a gravitational atomic cavity is a challenging alternative to Bose-Einstein condensation. It should have the advantage to reduce the collisional constraints. But one has first to find an efficient way of selecting such excited modes!

References

[1] J. Dalibard and C. Cohen-Tannoudji, J. Opt. Soc. Am. **B2** 1707 (1985)

[2] S. Chu, J. Bjorkholm, A. Ashkin and A. Cable, Phys. Rev. Lett. **57** 314 (1986)

[3] P. Gould, P. Lett, P. Julienne, W.D. Phillips, W. Thorsheim and J. Weiner, Phys. Rev. Lett. **60** 788 (1988)

[4] T. Hänsch and A. Schawlow, Opt. Commun. **13** 68 (1975)

[5] D. Wineland and H. Dehmelt, Bull. Am. Phys. Soc. **20** 637 (1975)

[6] S. Chu, L. Hollberg, J. Bjorkholm, A. Cable and A. Ashkin, Phys. Rev. Lett. **55** 48 (1985)

[7] D.J. Wineland and W.M. Itano, Phys. Rev. **A20** 1521 (1979)

[8] J.P. Gordon and A. Ashkin, Phys. Rev. A21 1606 (1980)

[9] E.L. Raab, M. Prentiss, A. Cable, S. Chu and D.E. Pritchard, Phys. Rev. Lett. 59 2631 (1987)

[10] P. Lett, R. Watts, C. Westbrook, W.D. Phillips, P. Gould and H. Metcalf, Phys. Rev. Lett. 61 169 (1988)

[11] P. Lett, W.D. Phillips, S. Rolston, C. Tanner, R. Watts and C. Westbrook, J. Opt. Soc. Am. B6 2084 (1989)

[12] J. Dalibard, C. Salomon, A. Aspect, E. Arimondo, R. Kaiser, N. Vansteenkiste and C. Cohen-Tannoudji, Atomic Physics 11, ed. S Haroche, J.C Gay and G. Grynberg (World Scientific, Singapour) p.199 (1989)

[13] Y. Shevy, D.S. Weiss, P.J. Ungar and S. Chu, Phys. Rev. Lett. 62 1118 (1989)

[14] D.S. Weiss, E. Riis, Y. Shevy, P.J. Ungar and S. Chu, J. Opt. Soc. Am. B6 2072 (1989)

[15] C. Salomon, J. Dalibard, W.D. Phillips, A. Clairon and S. Guellati, Europhys. Lett. 12 683 (1990)

[16] C. Gerz, T.W. Hodapp, P. Jessen, K.M. Jones, W.D. Phillips, C.J. Westbrook and K. Mølmer, Europhys. Lett. 21 661 (1993)

[17] J. Dalibard and C. Cohen-Tannoudji, J. Opt. Soc. Am. B6 2023 (1989)

[18] P.J. Ungar, D.S. Weiss, E. Riis and S. Chu, J. Opt. Soc. Am. B6 2058 (1989)

[19] C. Cohen-Tannoudji in "Fundamental systems in Quantum optics", Proceedings of the Session LIII of Les Houches Summer School, J. Dalibard, J.-M. Raimond and J. Zinn-Justin Editors, North-Holland (1992)

[20] Y. Castin, J. Dalibard, C. Cohen-Tannoudji, Proceedings of Light Induced Kinetic Effects, eds L. Moi, S. Gozzini, C. Gabbanini, E. Arimondo and F. Strumia (ETS Editrice, Pisa, 1991)

[21] Y. Castin and J. Dalibard, Europhys. Lett. 14 761 (1991)

[22] J.Y. Courtois, thèse de doctorat de l'École Polytechnique, Paris, France (1993)

[23] P. Verkerk, B. Lounis, C. Salomon, C. Cohen-Tannoudji, J.Y. Courtois, G. Grynberg, Phys. Rev. Lett. 68 3861 (1992)

[24] J.Y. Courtois and G. Grynberg, Phys. Rev. A46 7060 (1992)

[25] P.S. Jessen, C. Gerz, P.D. Lett, W.D. Phillips, S.L. Rolston, R.J.C. Spreeuw and C.I. Westbrook, Phys. Rev. Lett. **69** 49 (1992)

[26] K. Berg-Sørensen, Y. Castin, K. Mølmer and J. Dalibard, Europhys. Lett. **22** 663 (1993)

[27] Y. Castin, K. Berg-Sørensen, K. Mølmer and J. Dalibard, to appear in Fundamentals of Quantum Optics III, Ehlotzky ed., Springer-Verlag (1993)

[28] A. Hemmerich, Zimmerman and T.W. Hänsch, Europhys. Lett. **22** 89 (1993)

[29] A. Hemmerich and T.W. Hänsch, Phys. Rev. Lett. **70** 410 (1993)

[30] G. Grynberg, B. Lounis, P. Verkerk, J.Y. Courtois and C. Salomon, Phys. Rev. Lett. **70** 2249 (1993)

[31] A. Clairon, P. Laurent, A. Nadir, M. Drewsen, D. Grison, B. Lounis and C. Salomon, Proceedings of the 6th European Frequency and Time Forum, held at ESTEC, Noordwijk (ESA SP-340, June 1992)

[32] A.M. Steane and C.J. Foot, Europhys. Lett. **14** 231 (1991)

[33] A.M. Steane, M. Chowdhury and C.J. Foot, J. Opt. Soc. Am. **B9** 2142 (1992)

[34] C.D. Wallace, T.P. Dinneen, K.Y.N. Tan, A. Kumarakrishnan, P.L. Gould and J. Javanainen, to be published (1993)

[35] T. Walker, D. Sesko and C. Wieman, Phys. Rev. Lett. **64** 408 (1990)

[36] A.M. Smith and K. Burnett, J. Opt. Soc. Am. **B9** 1240 (1992)

[37] A. Gallagher and D.E. Pritchard, Phys. Rev. Lett. **63** 957 (1989)

[38] P.S. Julienne and J. Vigué, Phys. Rev. **44** 4464 (1991)

[39] A. Aspect, E. Arimondo, R. Kaiser, N. Vansteenkiste and C. Cohen-Tannoudji, Phys. Rev. Lett. **61** 826 (1988)

[40] A. Aspect, E. Arimondo, R. Kaiser, N. Vansteenkiste and C. Cohen-Tannoudji, J. Opt. Soc. Am. **B6** 2112 (1989)

[41] M. Kasevich and S. Chu, Phys. Rev. Lett. **69** 1741 (1992)

[42] H. Wallis and W. Ertmer, J. Opt. Soc. Am. **B6** 2211 (1989)

[43] K. Mølmer, Phys. Rev. Lett. **66** 2301 (1991)

[44] F. Bardou, J.P. Bouchaud, O. Emile, A. Aspect and C. Cohen-Tannoudji, submitted to Phys. Rev. Lett. (1993)

[45] F. Mauri, F. Papoff and E. Arimondo, Proceedings of Light Induced Kinetic Effects, eds L. Moi, S. Gozzini, C. Gabbanini, E. Arimondo and F. Strumia (ETS Editrice, Pisa, 1991)

[46] M.A. Ol'shanii and V.G. Minogin, Proceedings of Light Induced Kinetic Effects, eds L. Moi, S. Gozzini, C. Gabbanini, E. Arimondo and F. Strumia (ETS Editrice, Pisa, 1991)

[47] J.P. Bouchaud and A. Georges, Phys. Rep. **195** 125 (1990)

[48] B. Lounis, J. Reichel and C. Salomon, C. R. Acad. Sci. Paris, t.316, Série II, p.739 (1993)

[49] R. Cook and R. Hill, Opt. Comm. **43** 258 (1982)

[50] V. Balykin, V. Letokhov, Y. Ovchinikov and A. Sidorov, Phys. Rev. Lett. **60** 2137 (1988)

[51] M. Kasevich, D. Weiss and S. Chu, Opt. Lett. **15** 607 (1990)

[52] H. Wallis, J. Dalibard and C. Cohen-Tannoudji, Appl. Phys. **B54** 407 (1992)

[53] C. Aminoff, A. Steane, P. Bouyer, P. Desbiolles, J. Dalibard and C. Cohen-Tannoudji, to be published

[54] C. Aminoff, P. Bouyer and P. Desbiolles, C. R. Acad. Sci. Paris, t.316, Série II, p.1535 (1993)